Observation of a Liquid−Gas Phase Transition in Monolayers of Alkyltrimethylammonium Alkyl Sulfates Adsorbed at the Air/Water Interface

Imre Varga,*,† Tamás Keszthelyi,*,‡ Róbert Mészáros,† Orsolya Hakkel,‡ and Tibor Gilányi†

Department of Colloid Chemistry, Eötvös University, P.O. Box 32, H-1518 Budapest 112, Hungary, and Chemical Research Centre, P.O. Box 17, H-1525 Budapest, Hungary

Received: May 10, 2004; In Final Form: August 26, 2004

The equilibrium adsorption layers of symmetric chain alkyltrimethylammonium alkyl sulfates ($C_n^+ \cdot C_n^-$ for $n = 8, 12$) were investigated at the air/water interface by sum-frequency vibrational spectroscopy in the function of the bulk surfactant concentration. To ensure the surface purity of the solutions investigated, an improved version of the foam fractionation method was used for the purification of the constituent ionic surfactants and the surface purity of the solutions was also checked. In the monolayer of the $C_{12}^+ \cdot C_{12}^-$ surfactant, a two-dimensional first-order gas/liquid phase transition was observed. At surfactant bulk concentrations just exceeding the concentration corresponding to the phase transition, the monolayer is conformationally disordered, liquidlike, but with increasing bulk surfactant concentration the conformational order of the monolayer increases. The SFG spectra of the $C_8^+ \cdot C_8^-$ monolayer did not indicate the occurrence of phase transition at room temperature.

Introduction

The phase behavior of Langmuir (insoluble) monolayers spread at the air/water interface has been widely investigated since their description by Pockels[1] and Langmuir.[2] Several different phases have been identified, and their characteristic features and structures are still the subject of intensive scientific research.[3] On the other hand, the phase behavior of adsorbed equilibrium (Gibbs) monolayers remained a controversial area until recent years. A few research groups observed a kink in the surface tension isotherms of certain soluble surfactants and interpreted these results as evidence for a first-order phase transition in the monolayer.[4]

However, these results could be disputed from two points of view. On one hand, a first-order phase transition is indicated by a break (a sudden change in slope) in the surface tension isotherm ($\gamma-\ln c$ function). Unfortunately, due to the experimental error of the surface tension measurements, it is very difficult to present convincing evidence that there is an actual break in the experimentally determined surface tension isotherms and not only a rapid change of the slope is observed.

On the other hand, the surface tension isotherm of water-soluble surfactants can be strongly affected by the presence of highly surface-active impurities. Thus, if the surface purity of the investigated system is not tested, it can always be argued that even if there is a kink in the surface tension isotherm it is due to the presence of highly surface-active impurities and not a characteristic feature of the investigated surfactant.[5]

In the past decade, several new or improved methods (ellipsometry,[6,7] X-ray diffraction,[8] neutron reflection,[9] sum-frequency vibrational spectroscopy[10−15]) became available in the research of surfactant monolayers, and by now the existence of solid/liquid[6,8,11,13−15] and liquid/gas[7] phase transitions in Gibbs monolayers is well-established. Particular attention was paid to the investigation of the monolayers of medium-chain alcohols. The existence of a solid/liquid-phase transition was demonstrated first by ellipsometry at the air/solution interface.[6] Subsequent X-ray diffraction studies indicated that the solid phase has a hexagonal unit cell and that the alkyl chains are oriented perpendicular to the water surface.[8] Subsequent investigations by sum-frequency vibrational spectroscopy showed[11] that the alkyl chains mainly adopt an all-trans conformation in the solid phase. When the monolayer melts, the area per molecules somewhat increases in the monolayer (∼10%), the average molecular tilt increases (from 0° to 18° with respect to the surface normal), and there is also a certain increase in the conformational disorder. Later the existence of solid/liquid-phase transition at the solid/liquid interface[12] and the existence of a gas/liquid-phase transition at the air/water interface[7] were also demonstrated. The investigations were also extended to the mixed monolayer of dodecanol−ionic surfactant (sodium dodecyl sulfate[9b,13] and alkyltrimethylammonium bromides[14]) and ionic surfactant−alkane (hexadecyltrimethylammonium bromide and tetradecane[15]) systems at the air/water interface. The observation of the solid/liquid-phase transition in these systems emphasized the dramatic effect of highly surface-active impurities on the adsorption properties of other surface-active molecules.

Recently, the existence of a gas/condensed type phase transition in the adsorption layers of catanionic surfactants and 1:1 oppositely charged surfactant mixtures has also been suggested.[16,17] The catanionic surfactants are defined as salts of an amphiphilic anion with an amphiphilic cation.[18] An essential feature of the catanionic surfactants is their very strong surface-active character.[19] The adsorption behavior of these solutions is special because both the cation and the anion may be accommodated in the monolayer and in the diffuse electric double layer as well. There are only a few works in this field,

* Corresponding authors. E-mail: imo@para.chem.elte.hu (I.V.), ktamas@sunserv.kfki.hu (T.K.).
† Eötvös University.
‡ Chemical Research Centre.

10.1021/jp048006o CCC: $30.25
Published on Web 12/16/2004

because of the experimental difficulties due to the low solubility of the catanionic surfactants. Many more publications deal with the surface behavior of the mixtures of aqueous cationic and anionic surfactant solutions because of the practical application of surfactant mixtures as detergents, dispersants, etc. It has been concluded that the 1:1 mixtures usually show behavior similar to the aqueous solutions of catanionic surfactants; thus they have extremely strong surface-active character as compared to that of the individual surfactants.[17,20,21] It has also been shown that the equimolar mixtures of symmetric chain cationic and anionic surfactants form an equimolar adsorption layer.[21,22] Recently, Matsuki et al. found that a two-dimensional gas/condensed type phase transition may take place in the case of mixtures of decyltrimethylammonium bromide and sodium decyl sulfate solutions due to the strong interactions of the surfactant ions in the adsorption layer.[17]

Lately, we have investigated the adsorption of symmetric chain catanionic surfactants (alkyltrimethylammonium alkyl sulfates; $C_n^+ \cdot C_n^-$ for $n = 8, 10, 12$) at the air/water interface by equilibrium and dynamic surface tension measurements.[16] The results of these measurements could be interpreted in terms of a two-dimensional gas/liquid-phase transition taking place in the adsorbed monolayer of the longer chain length ($n = 10, 12$) surfactants. In the case of the octyltrimethylammonium octyl sulfates, the phase transition could not be observed. We have also proposed a molecular interaction model to describe the surface behavior of the investigated catanionic surfactants. The model successfully predicted that phase transition occurs only in the case of the longer chain length surfactants ($n = 10, 12$). This trend could be attributed to the fact that with increasing chain length the attractive interactions in the monolayer increased much more in the case of the liquid phase than in the case of the gas phase, which made the formation of the liquid phase more favorable as compared to the gas phase in the case of the longer chain length surfactants (for further details, see ref 16).

Because our investigations were based on surface tension measurements, the existence of the observed break in the equilibrium surface tension isotherms and thus the occurrence of the two-dimensional phase transition could also be disputed. In this work, we use infrared-visible sum-frequency spectroscopy (SFS) as an independent method to investigate the phase behavior of the above surfactants. Sum-frequency vibrational spectroscopy is a second-order nonlinear optical technique that, due to its inherent surface specificity, has been widely used for the investigation of interfacial phenomena.[23] The SFS results presented here provide very strong support to our previous observation of the two-dimensional phase transition in the adsorbed monolayer of the $n = 10$ and $n = 12$ surfactants.

We also demonstrate the surface purity of the investigated systems to exclude the possibility that the observed phase transition could be attributed to the presence of highly surface-active impurities (alcohols).

Experimental Section

Materials. Because previously we have found that the presence of an inert electrolyte does not affect the occurrence of the two-dimensional phase transition,[16] for the sake of simplicity we used 1:1 mixtures of sodium alkyl sulfates and alkyltrimethylammonium bromides in these investigations. The anionic surfactants (sodium dodecyl sulfate and sodium octyl sulfate) were ordered from Merck (Darmstadt, Germany), while the cationic surfactants (dodecyltrimethylammonium bromide and octyltrimethylammonium bromide) were purchased from Sigma (Germany). Both the anionic and the cationic surfactants were recrystallized twice before their further use. The anionic surfactants were recrystallized from a 1:1 mixture of benzene and ethanol, while the cationic surfactants were recrystallized from a 1:4 mixture of ethanol and acetone.

Prior to the preparation of the 1:1 cationic/anionic surfactant mixtures, the aqueous solutions of the constituent ionic surfactants were purified by an improved version of the foam fractionation method. To improve the efficiency of the method, we used microbubbles instead of the commonly used macrobubbles. Microbubbles were generated by pressing nitrogen through a G-5 sintered glass filter into the solution. The solution was stirred, and the foam formed above the solution was continuously removed. The purification procedure took 1 h. The concentration change of the surfactant solutions was monitored by means of electrical conductivity measurements, and the surface purity of the resulting solutions was checked (see below). Stock solutions of the 1:1 cationic/anionic surfactant mixtures were prepared from the foam fractionated surfactant solutions. Surface tension and SFS measurements were carried out on solutions prepared by further dilution of the previously prepared stock solutions. The stock solutions of the cationic/anionic surfactant mixtures were always used only on the day of their preparation.

Pendant Drop Measurements. Pendant drop measurements were used for the monitoring of the surface tension relaxation of the surfactant solutions. The applied apparatus consisted of a lighting system, a drop-forming system, a sample holder chamber, and an image forming and recording system. The lighting system consisted of a halogen lamp and appropriate optics to produce a uniformly lit background behind the pendant drop. The pendant drops were formed at the tip of a Teflon capillary ($r = 1.853 \pm 0.001$ mm) which joined a gastight Hamilton syringe placed in a computer-controlled syringe pump. The drops were formed in a closed, temperature-controlled chamber (having an internal size: $1.0 \times 2.0 \times 5.0$ cm). To avoid the evaporation of the pendant drop, the sidewalls of the chamber were covered with wetted filter paper (the volume decrease of the drop did not exceed 1−2% during 1 h). The image of the pendant drop was formed by the objective on the sensor of a CCD camera, which transmitted the signal to a frame grabber (Firstsight Vision, Falcon) installed in a personal computer. The frame grabber produced a digital image of the pendant drop having 768×576 resolution and eight-bit gray color depth. Finally, the contour of the pendant drop was determined from the digital image by an edge detection routine.

The shape (contour) of a pendant drop is determined by the Laplace equation:

$$\Delta p = \gamma\left(\frac{1}{R_1} + \frac{1}{R_2}\right)$$

where γ is the surface tension, R_1 and R_2 are the two principal radii of curvature of the surface, and Δp is the pressure difference across the interface. This equation can be rewritten as a set of three first-order differential equations[24,25] and fitted to the experimental contour of the pendant drop. As the result of the fitting procedure, the surface tension of the pendant drop can be determined.

The applied experimental procedure was as follows: By turning on the syringe pump, a series of drops were formed at the tip of the capillary, thus ensuring the creation of a clean surface. The time required for the formation of a pendant drop was approximately 1 s. After the formation of the third pendant drop, the syringe pump was stopped and the monitoring of the

drop shape started ($t = 0$). A picture of the pendant drop was taken every 5 s, and then the recorded sequential digital images were used for the calculation of the temporary surface tension values giving rise to the surface tension versus relaxation time function. The accuracy and reproducibility of the determined surface tension values were ~0.1 mN/m.

Sum-Frequency Spectroscopy. Sum-frequency spectra were collected by an EKSPLA[26] (Vilnius, Lithuania) SFG spectrometer. The visible beam (532 nm) is generated by doubling the fundamental output of a Nd:YAG laser (1064 nm wavelength, 20 ps pulse width, 20 Hz repetition rate). The tuneable IR beam is obtained from an optical parametric generation/difference frequency generation system, pumped by the third harmonic and the fundamental of the Nd:YAG laser. The IR and visible beams are temporally and spatially overlapped on the sample surface with incident angles of 55° and 60°, respectively. The beam energies at the sample were kept at 200 μJ. Sum frequency light is collected in the reflected direction through a holographic notch filter and monochromator and is detected by a PMT. Spectral resolution is determined by the ~6 cm^{-1} line width of the IR pulse. All spectra presented were collected using the ssp polarization combination (s-polarized sum-frequency, s-polarized visible, and p-polarized IR radiation). Spectra were collected in the 2800−3000 cm^{-1} spectral region using 3 cm^{-1} increments and 50 laser pulses at each step. Typically, seven such spectra were collected and averaged at each surfactant concentration, and the measurements at each concentration were repeated on 2−3 different days. The surfactant solutions were contained in 25 mm inner diameter, 30 mm tall Teflon cells, and kept at 23 °C.

Results and Discussion

Surface Purity. To measure reliable surface tension data, one must ensure the surface purity of the sample investigated. This is a serious problem in the case of ionic surfactants because they contain impurities (mainly alkanols and longer chainlength homologues) that are far more surface active than the ionic surfactant investigated. This means that components that are present only in traces in the bulk phase can become a major constituent of the adsorption layer[13,14,27] and thus have a profound effect on the equilibrium surface tension of the solution. Therefore, the purification of the surfactant solution and the test of the surface purity are essential requirements if the surface properties of the two-component (ionic surfactant/water) system are to be described.

As it is described in the Experimental Section, an improved version of the foam fractionation method was used to purify the surfactant solutions. However, in the case of the catanionic surfactant solutions, the direct foam fractionation of the solution would give rise to the removal of the surfactant from the bulk phase due to the extreme low bulk surfactant concentration (the solubility of the dodecyltrimethylammonium dodecyl sulfate is ~2×10^{-5} mol/dm^3). To avoid this possibility and to ensure the surface purity of the system, the solutions of the constituent surfactants were purified.

The surface purity of the resulting solutions was tested by dynamic surface tension measurements. In Figure 1, the dynamic surface tension curves of 4.0 mM sodium dodecyl sulfate and 4.0 mM dodecyltrimethylammonium bromide solutions can be seen, prepared both from foam fractionated and from unpurified stock solutions. The slow surface tension change of the unpurified solutions clearly indicates that these solutions are not in equilibrium due to the slow diffusion of highly surface-active impurities from the bulk phase to the adsorption layer.

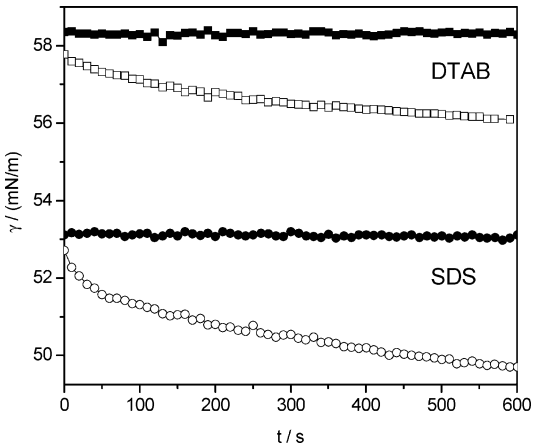

Figure 1. Dynamic surface tension curves of 4.0 mM SDS (circles) and DTAB (squares) solutions. The solid symbols denote samples that were foam fractionated, while the open symbols denote samples that were not purified.

However, as it is demonstrated in Figure 1, the surface tension of the purified solutions is practically constant. This means that the equilibrium adsorption layer could be established due to the removal of the surface-active impurities by the purification procedure.

Sum-Frequency Spectroscopy. Sum-frequency spectroscopy measurements were performed on 1:1 mixtures of octyltrimethylammonium bromide and sodium octyl sulfate ($C_8^+ \cdot C_8^-$) as well as for 1:1 mixtures of dodecyltrimethylammonium bromide and sodium dodecyl sulfate ($C_{12}^+ \cdot C_{12}^-$) at the air/water interface as a function of bulk surfactant concentration. The $C_8^+ \cdot C_8^-$ surfactant mixture was chosen because it could be used as a reference system since it was known from previously done surface tension measurements that phase transition does not occur in its adsorption layer.[16] Selected ssp sum-frequency spectra are plotted in Figure 2a and b.

Assignment. The assignment of the major peaks in the spectra is well established in the literature.[28] The peak at 2852 cm^{-1} arises from the symmetric methylene stretch (d^+ mode). The peak at 2878 cm^{-1} is attributed to the symmetric methyl stretch (r^+ mode), and a Fermi resonance of the same mode is observed at 2940 cm^{-1} (r_{FR}^+). The two components (in-plane, r_a^-, and out-of-plane, r_b^-) of the asymmetric methyl stretch are observed as a shoulder at ~2960 cm^{-1}. Finally, the broad envelope centered at 2925 cm^{-1} contains the antisymmetric methylene stretch and a Fermi resonance of the symmetric methylene stretch.

As the SF spectra indicate, the two systems investigated have essentially different surface behavior. In the case of the $C_8^+ \cdot C_8^-$ mixtures, the peaks are slowly emerging from the noise level as the bulk surfactant concentration increases. On the other hand, in the case of the $C_{12}^+ \cdot C_{12}^-$ mixtures, the peaks abruptly appear when the bulk surfactant concentration is increased from 6.31 $\times 10^{-7}$ to 7.08 $\times 10^{-7}$ mol/dm^3 ($\Delta c = 7.7 \times 10^{-8}$ mol/dm^3). In Figure 2c and d, the fitting amplitudes (A_q, see below) of the symmetric methyl ($A[r^+]$) and methylene ($A[d^+]$) modes are plotted as a function of the bulk surfactant concentration. The figures clearly show that the amplitudes of both peaks continuously change in the case of the $C_8^+ \cdot C_8^-$ surfactant, while there is a sharp intensity step in the case of the $C_{12}^+ \cdot C_{12}^-$ surfactant.

Background. According to the basic theory of sum-frequency generation,[23a,29] the sum-frequency intensity in the reflected direction is proportional to the square of the nonlinear susceptibility, $\chi^{(2)}$. The susceptibility, in turn, is related to the molecular

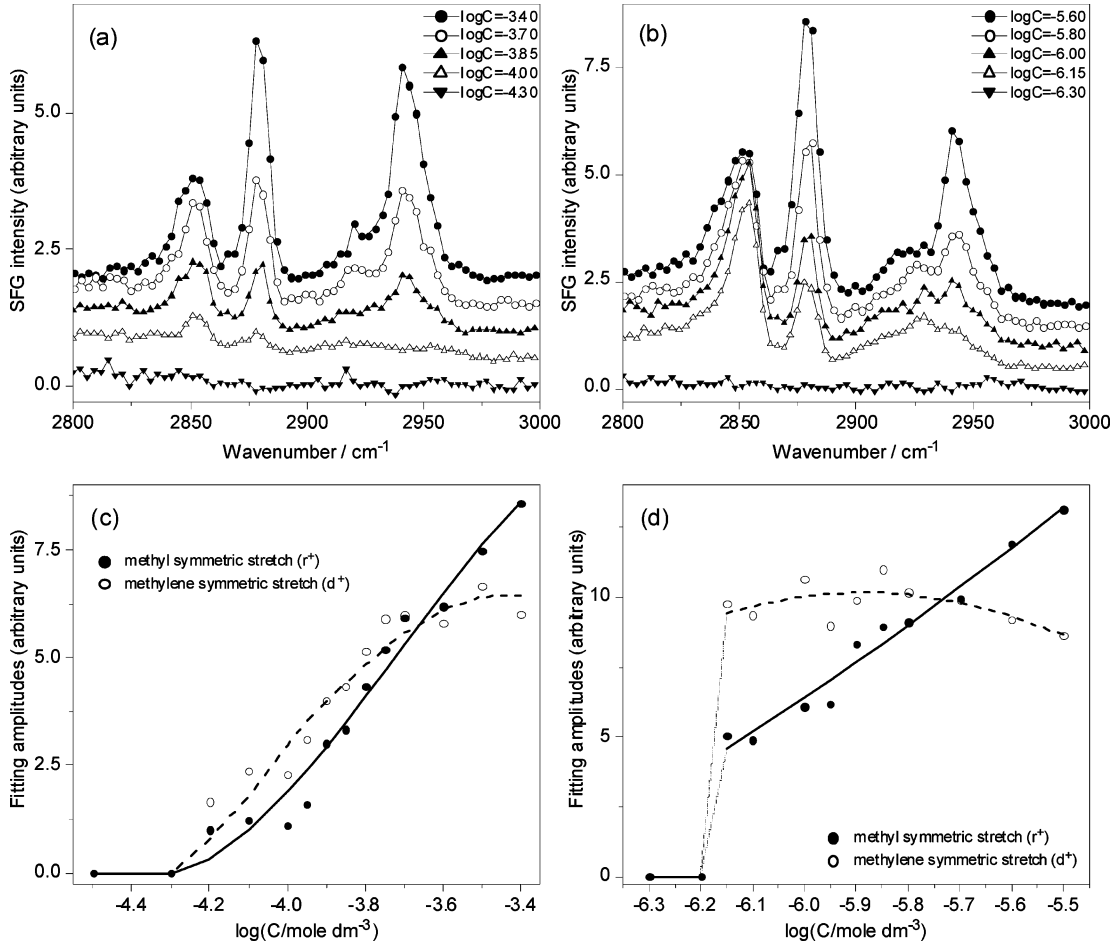

Figure 2. (a) Sum-frequency ssp spectra of $C_8^+ \cdot C_8^-$ for five different bulk surfactant concentrations ranging from 5.01×10^{-5} to 3.98×10^{-4} mol/dm^3. Symbols are measured data points; solid lines are a guide to the eye. The spectra have been vertically displaced for clarity. (b) Sum-frequency ssp spectra of $C_{12}^+ \cdot C_{12}^-$ for five different bulk surfactant concentrations ranging from 5.0×10^{-7} to 3.16×10^{-6} mol/dm^3. Symbols are measured data points; solid lines are a guide to the eye. The spectra have been vertically displaced for clarity. (c) Fitting amplitudes of the methyl symmetric stretch (r^+, at 2878 cm^{-1}, ●) and methylene symmetric stretch (d^+, at 2852 cm^{-1}, ○) modes in the ssp sum-frequency spectra of $C_8^+ \cdot C_8^-$ for 14 different bulk surfactant concentrations investigated. The lines are only a guide to the eye. (d) Fitting amplitudes of the methyl symmetric stretch (r^+, at 2878 cm^{-1}, ●) and methylene symmetric stretch (d^+, at 2852 cm^{-1}, ○) modes in the ssp sum-frequency spectra of $C_{12}^+ \cdot C_{12}^-$ for 12 different bulk surfactant concentrations investigated. The lines are only a guide to the eye.

hyperpolarizability, $\beta^{(2)}$, through the relation:

$$\chi_{ijk}^{(2)} = N_s \sum_{a,b,c} \langle \Omega_{abc,ijk} \rangle \beta_{abc}^{(2)} \quad (1)$$

where the term in brackets denotes an average over the molecular orientational distribution, and N_s is the number density of the surface molecules. For an azimuthally isotropic liquid interface under the ssp polarization combination used in the present work, only the χ_{yyz} component of the second-order susceptibility tensor contributes to the effective nonlinear susceptibility. Assuming C_{3v} symmetry for the methyl group, there are only two independent nonvanishing components of the hyperpolarizability for the symmetric stretch mode, $\beta_{aac} = \beta_{bbc}$, and β_{ccc}, and the above equation reduces to:

$$\chi_{yyz}^{(2)} = \frac{1}{2} N_s \beta_{ccc} [\langle \cos\theta \rangle (1 + r) - \langle \cos^3\theta \rangle (1 - r)] \quad (2)$$

where $r = \beta_{aac}/\beta_{ccc}$, and θ is the polar angle (tilt) between the symmetry axis, c (the C_3 axis of the methyl group), and the laboratory z axis (the surface normal). From eq 2, it is seen that the strength of the symmetric methyl stretch mode in the ssp spectrum decreases as the average molecular tilt increases.

We modeled the ssp sum-frequency spectra applying the usual expression:

$$\chi_{yyz}^{(2)}(\omega) = A_{NR} e^{i\varphi} + \sum_q \frac{A_q}{\omega - \omega_q + i\Gamma_q} \quad (3)$$

where A_q, ω_q, and Γ_q are the amplitude, resonant frequency, and damping constant, respectively, of the qth vibrational normal mode, while A_{NR} and φ are the amplitude and phase of the nonresonant contribution.

Sum-frequency spectra are also very sensitive to the conformation of the alkyl chains, as in the case of an all-trans chain, the methylene modes (d^+, d^-, and d^+_{FR}) are SF-inactive due to their local centrosymmetry. The presence of the methylene modes in sum-frequency spectra is generally taken as an indication of gauche defects in the alkyl chains, and in fact the amplitude ratio of the symmetric methylene and methyl modes ($A[d^+]/A[r^+]$) is often taken as a measure of the conformational order of alkyl chains.[30]

The $C_8^+ \cdot C_8^-$ Surfactant. The observed peak intensity changes can thus be interpreted in terms of the change of the adsorbed amount accompanied by the orientation and conformation changes of the alkyl chains. Because phase transition does

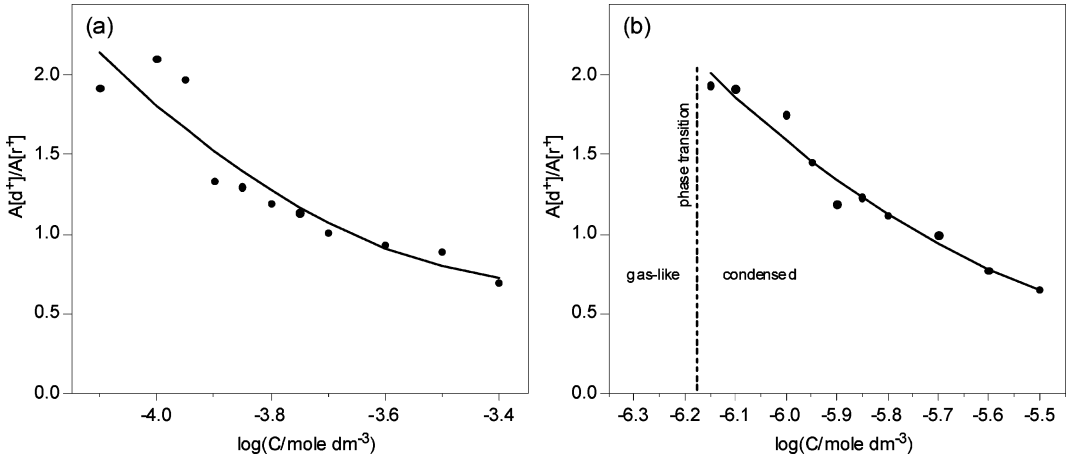

Figure 3. (a) Ratio of the fitting amplitudes of the methylene symmetric stretch and methyl symmetric stretch modes ($A[d^+]/A[r^+]$), plotted as a function of the bulk surfactant concentration for the $C_8^+ \cdot C_8^-$ surfactant. The solid line is only a guide to the eye. (b) Ratio of the fitting amplitudes of the methylene symmetric stretch and methyl symmetric stretch modes ($A[d^+]/A[r^+]$), plotted as a function of the bulk surfactant concentration for the surfactant. The solid line is only a guide to the eye.

not occur in the monolayer of the $C_8^+ \cdot C_8^-$ surfactant at room temperature,[16] the surface excess of this surfactant must continuously increase as the bulk concentration increases and the peak intensities should continuously increase with the bulk surfactant concentration if the adsorbed amount of the surfactant was the only factor governing them. However, the peak intensities are also affected by the orientation and conformation of the alkyl chains.

As mentioned above (eq 2), the strength of the symmetric methyl stretch in the ssp spectrum increases as the average molecular tilt decreases. Taking into account that the average tilt of the surfactant alkyl chains decreases as the adsorbed amount increases, it can be concluded that both the increasing adsorbed amount and the chain orientation change contribute to the increase of the intensity of the methyl symmetric stretch peak at 2878 cm^{-1} as the bulk surfactant concentration increases.

On the other hand, the intensity of the methylene symmetric stretch peak at 2852 cm^{-1} first increases and then becomes practically constant in the function of the bulk surfactant concentration (Figure 2c). This means that a decreasing contribution from the hyperpolarizability must compensate the increasing contribution of the surface concentration. Because the alkyl chains being in all-trans conformation are SF-inactive, the observation may be interpreted in terms of the relative abundance of this conformation in the adsorption layer. It was found recently by Monte Carlo simulations of octane adsorption layers at the water/vapor interface that the alkyl chains prefer the all-trans conformation lying parallel to the interface at low surface coverage (approximately 30% of the adsorbed molecules adopted this conformation[31]). Nevertheless, as the surface concentration increases and the adsorbed molecules start to overlap each other, the fraction of the all-trans alkyl chains decreases. Assuming that similar conformation changes occur at low adsorbed amounts in a surfactant adsorption layer, the conformation changes of the alkyl chains may also contribute to the intensity increase of the symmetric methylene mode in the ssp spectrum at small surfactant concentrations. However, as the surface concentration further increases, the area per surfactant molecules decreases, and thus the alkyl chains become more stretched by decreasing the number of SF-active gauche conformations. As a consequence, the ensemble averaged hyperpolarizability should decrease with increasing bulk surfactant concentration, giving a decreasing contribution to the SF-intensity of the symmetric methylene mode in the ssp spectra.

The $C_{12}^+ \cdot C_{12}^-$ Surfactant. In the case of the $C_{12}^+ \cdot C_{12}^-$ surfactant, the bulk surfactant concentration dependence of the SF-intensities is quite different from those of the $C_8^+ \cdot C_8^-$ surfactant. In this case, the peaks abruptly appear due to a small increase in the bulk surfactant concentration (Figure 2d). However, it may be argued that because the adsorption of the $C_{12}^+ \cdot C_{12}^-$ surfactant is a slow process, allowing more time for the adsorption, the appropriate SF-spectra would appear in the low concentration range. To avoid this possibility, the time allowed for the adsorption of the surfactant before the SF-measurements was determined following the reasoning of Bain et al.[7] The surfactant molecules of the monolayer must come from the bulk solution from the close vicinity of the interface. As a consequence, this region is depleted in surfactant molecules. If the surface concentration of the surfactant is Γ and the average decrease of the surfactant concentration in the depletion region is Δc, then the thickness of the depleted region is: $h \approx \Gamma/\Delta c$. The time required for the surfactant molecules to travel through this region can be given as

$$t = \frac{1}{2D}\left(\frac{\Gamma}{\Delta c}\right)^2 \tag{4}$$

where D is the diffusion coefficient of the surfactant. Assuming that the concentration decrease of the depletion region is proportional to the bulk surfactant concentration (c), the ratio of the diffusion times in two different concentration surfactant solutions can be given as $t_1/t_2 = (\Gamma_1/\Gamma_2)^2(c_2/c_1)^2$. If we further assume that $\Gamma_1 = \Gamma_2$, an upper limit can be given for the diffusion time in the less concentrated solution in terms of the bulk surfactant concentrations. Using the concentrations of the surfactant solutions before and after the observed intensity jump in the SF-intensities ($c_1 = 6.31 \times 10^{-7}$ mol/dm^3, $c_2 = 7.08 \times 10^{-7}$ mol/dm^3, respectively), a value of 1.25 can be determined for the ratio of the two diffusion times. Because the SF-measurements were carried out less than 1 h after the creation of the fresh surface at c_2, the required diffusion time is estimated to be less than 75 min at c_1. However, considering the semiquantitative nature of this estimation, 3 h was allowed to pass after the creation of the fresh surface at c_1, thereby excluding the possibility that the observation of the intensity jump is only an experimental artifact.

The observed intensity jump of the SF-spectra should indicate an abrupt change in the adsorption layer. In principle, this change may reflect either the discontinuous increase of the

surface concentration or an abrupt change in the chain orientation and conformation at approximately constant surface coverage. However, the latter case means that a considerable amount of surfactant must accumulate at the surface before the conformation change takes place without contributing to the resonant peaks of the SF spectrum. This would only be possible if all of the alkyl chains were in the all-trans conformation in the adsorption layer with the molecules lying parallel with the surface. Although such a situation could be favored energetically, it is entropically highly unfavorable. This is also reflected by Monte Carlo simulations, which indicate that even at low surface coverage only a portion of the molecules adopt this orientation and conformation.[31] Thus, it can be concluded that an abrupt surface concentration increase must have a considerable role in the observed sudden peak intensity increase of the SF-spectra, which indicates that a first-order gas/condensed phase transition takes place in the adsorption layer.

Conformational Order of the Alkyl Chains. As we already noted, the relative intensity of the methylene and methyl symmetric stretch modes in an ssp spectrum is often used as a measure of the conformational order of the hydrocarbon chains. In the case of perfect order, this ratio is zero, and as conformational order decreases, this quantity increases. To address the question of conformational order in the adsorption layer, we plot the $A[d^+]/A[r^+]$ ratio of the fitting amplitudes for the methylene and methyl symmetric stretch modes as a function of the bulk surfactant concentration in Figure 3.

The calculated methylene to methyl amplitude ratios are only physically meaningful when the SFG signal (and thus the fitting amplitudes) is different from zero. In the case of the $C_{12}^+ \cdot C_{12}^-$ surfactant, this means that the ratio can only be calculated for concentrations exceeding that corresponding to the formation of the condensed phase.

At the lowest concentrations, a relatively large value is calculated for the ratio ($\sim$2) in the case of both surfactants, which decreases as the bulk surfactant concentration increases. The large ratios indicate that the developing monolayers contain a substantial conformational disorder not only in the case of the $C_8^+ \cdot C_8^-$ surfactant where the adsorbed amount continuously increases but also in the case of the $C_{12}^+ \cdot C_{12}^-$ surfactant where a condensed phase appears after the phase transition. This suggests that the condensed phase formed after the phase transition in the adsorption layer of the $C_{12}^+ \cdot C_{12}^-$ surfactant is liquidlike. As the bulk surfactant concentration increases, the calculated ratios are decreasing. This indicates that the conformational disorder in the monolayers decreases with the ongoing adsorption of the surfactant molecules due to the compression of the adsorption layer.

Summary

Using sum-frequency spectroscopy, we have investigated the surface behavior of surface chemically pure dodecyltrimethylammonium dodecyl sulfate and octyltrimethylammonium octyl sulfate solutions at the air/solution interface.

The physical picture proposed for the interpretation of the experimental results (surface tension data and SFG measurements) can be summarized in the scheme presented in Figure 4. The surface behavior of the $C_8^+ \cdot C_8^-$ surfactant corresponds to that of an ordinary surfactant. At low enough chemical potential (bulk surfactant concentrations), a gaslike monolayer develops in which the interaction of the adsorbed surfactant molecules is negligible (Figure 4b). With increasing chemical potential (bulk surfactant concentration), the adsorbed amount

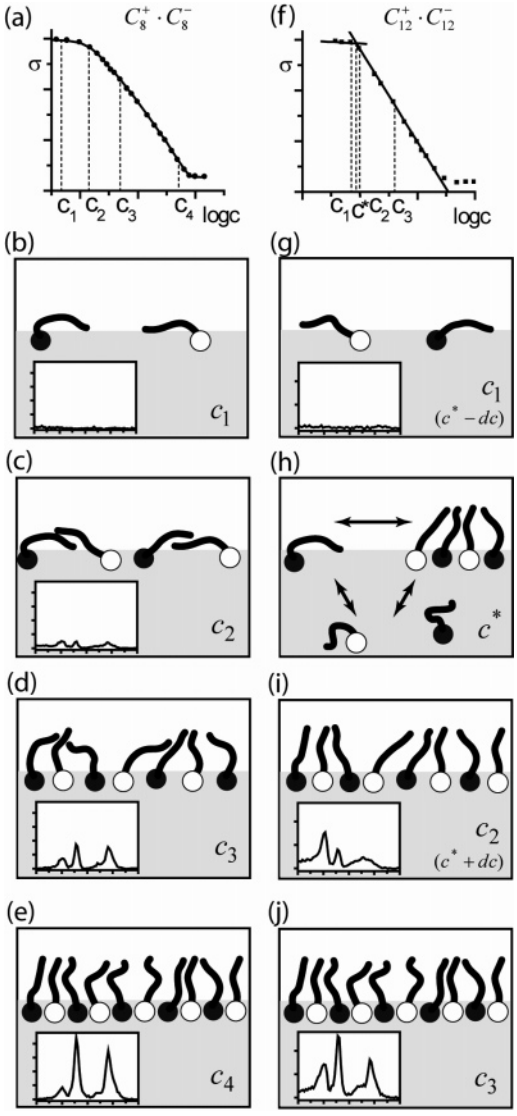

Figure 4. Schematic illustration of the physical picture proposed for the interpretation of the experimental results for the $C_8^+ \cdot C_8^-$ surfactant (a−e), and the $C_{12}^+ \cdot C_{12}^-$ surfactant (f−j). (a) and (f) are the equilibrium surface tension versus bulk concentration curves adapted from ref 16. (b−e) and (g−j) illustrate the evolution of the adsorption layer as the bulk surfactant concentration is increased for the $C_8^+ \cdot C_8^-$ and $C_{12}^+ \cdot C_{12}^-$ surfactants, respectively. Insets show the sum-frequency spectra measured at the corresponding concentration.

continuously increases, leading to the continuous development of a dense monolayer (Figure 4c−e). This is indicated by the continuously changing curvature of the equilibrium surface tension versus concentration curve (Figure 4a) and the gradually appearing SFG spectra with increasing bulk surfactant concentration.

On the other hand, the $C_{12}^+ \cdot C_{12}^-$ surfactant exhibits a qualitatively different surface behavior. At low enough chemical potential (bulk surfactant concentration), a gaslike surfactant monolayer forms (Figure 4g). As the chemical potential increases, at a given chemical potential value, a liquidlike phase appears in equilibrium with the gaslike phase in the monolayer. At the bulk concentration corresponding to this chemical potential value (c^*), a three-phase equilibrium exists (the bulk solution is in equilibrium with the gaslike and the liquidlike phases of the monolayer; see Figure 4h). The equilibrium chemical potential of the system (and the equilibrium bulk surfactant concentration) can only increase further if the whole monolayer turns into the liquidlike phase (dense monolayer;

Figure 4i). The monolayer turns from a gaslike phase to a liquidlike dense phase at a constant chemical potential, which means that a first-order phase transition takes place in the adsorption layer. The occurrence of the phase transition is indicated by the breakpoint in the equilibrium surface tension versus concentration curve at c^* (Figure 4f) and by the sudden increase of the SFG intensities at the same bulk surfactant concentration. With further increasing chemical potential (bulk surfactant concentration), the liquidlike phase is compressed (Figure 4j) as is indicated by the increasing conformational order of the monolayer.

Acknowledgment. This work was supported by the Hungarian Scientific Research Fund (OTKA No. F 034838 and T 047368) and by the Ministry of Education (FKFP 0051/2001).

References and Notes

(1) Pockels, A. *Nature* **1891**, *43*, 437.
(2) Langmuir, I. *J. Am. Chem. Soc.* **1917**, *39*, 1848.
(3) Kaganev, V. M.; Möhwald, H.; Dutta, P. *Rev. Mod. Phys.* **1999**, *71*, 779.
(4) (a) Aratono, M.; Uryu, S.; Hayami, Y.; Motomura, K.; Matuura, R. *J. Colloid Interface Sci.* **1984**, *98*, 33. (b) Lin, S. Y.; McKeigue, K.; Maldarelli, C. *Langmuir* **1991**, *7*, 1055. (c) Lin, S. Y.; Lu, T. L.; Hwang, W. B. *Langmuir* **1995**, *11*, 555. (d) Lin, S. Y.; Tsay, R. Y.; Hwang, W. B. *Colloids Surf., A* **1996**, *114*, 131. (e) Lin, S. Y.; Hwang, W. B.; Lu, T. L. *Colloids Surf., A* **1996**, *114*, 143.
(5) Hirte, R.; Lunkenheimer, K. *J. Phys. Chem.* **1996**, *100*, 13786−13793.
(6) Berge, B.; Renault, A. *Europhys. Lett.* **1993**, *21*, 773.
(7) Casson, B. D.; Bain, C. D. *J. Am. Chem. Soc.* **1999**, *121*, 2615−2616.
(8) (a) Renault, A.; Legrand, J. F.; Goldmann, M.; Berge, B. *J. Phys. II* **1993**, *3*, 761. (b) Berge, B.; Konovalov, O.; Lajzerowicz, J.; Renault, A.; Rieu, J. P.; Vallade, M.; Als-Nielsen, J.; Grübel, G.; Legrand, J. F. *Phys. Rev. Lett.* **1994**, *73*, 1652−1655. (c) Legrand, J. F.; Renault, A.; Konovalov, O.; Chevigny, E.; Als-Nielsen, J.; Grubel, G.; Berge, B. *Thin Solid Films* **1994**, *248*, 95−99. (d) Rieu, J. P.; Legrand, J. F.; Renault, A.; Berge, B.; Ocko, B. M.; Wu, X. Z.; Deutsch, M. *J. Phys. II* **1995**, *5*, 607−619.
(9) (a) Penfold, J.; Thomas, R. K.; Simister, E.; Lee, E.; Rennie, A. *J. Phys.: Condens. Matter* **1990**, *2*, SA411−SA416. (b) Lu, J. R.; Purcell, I. P.; Lee, E. M.; Simister, E. A.; Thomas, R. K.; Rennie, A. R.; Penfold, J. *J. Colloid Interface Sci.* **1995**, *174*, 441−455.
(10) Bell, G. R.; Bain, C. D.; Ward, R. N. *J. Chem. Soc., Faraday Trans.* **1996**, *92*, 515−523.
(11) (a) Braun, R.; Casson, B. D.; Bain, C. D. *Chem. Phys. Lett.* **1995**, *245*, 326−334. (b) Casson, B. D.; Braun, R.; Bain, C. D. *Faraday Discuss.* **1996**, *104*, 209.
(12) Johal, M. S.; Usadi, E. W.; Davies, P. B. *J. Chem. Soc., Faraday Trans.* **1996**, *92*, 573−578.
(13) Casson, B. D.; Bain, C. D. *J. Phys. Chem. B* **1998**, *102*, 7434−7441.
(14) Casson, B. D.; Bain, C. D. *J. Phys. Chem. B* **1999**, *103*, 4678−4686.
(15) McKenna, C. E.; Knock, M. M.; Bain, C. D. *Langmuir* **2000**, *16*, 5853−5855.
(16) Gilányi, T.; Mészáros, R.; Varga, I. *Langmuir* **2000**, *16*, 3200−3205.
(17) Matsuki, H.; Aratono, M.; Kaneshina, S.; Motomura, K. *J. Colloid Interface Sci.* **1997**, *191*, 120.
(18) Jokela, P.; Jönsson, B.; Sadaghiani, A. S.; Khan, A. *Langmuir* **1991**, *7*, 889.
(19) Hoyer, H. W.; Marmo, A.; Zoellner, M. *J. Phys. Chem.* **1961**, *65*, 1804. Corkill, J. M.; Goodman, J. F.; Ogden, C. P.; Tate, J. R. *Proc. R. Soc. London, Ser. A* **1963**, *273*, 83.
(20) Huang, J. B.; Zhao, G. X. *Colloid Polym. Sci.* **1995**, *273*, 156. Rodakiewicz-Novak, J. *J. Colloid Interface Sci.* **1981**, *84*, 532. Rodakiewicz-Novak, J. *J. Colloid Interface Sci.* **1982**, *85*, 586. Rodakiewicz-Novak, J. *Colloids Surf.* **1983**, *6*, 143.
(21) Góralczyk, D. *Colloid Polym. Sci.* **1994**, *272*, 204. Góralczyk, D. *J. Colloid Interface Sci.* **1994**, *167*, 172. Góralczyk, D. *J. Colloid Interface Sci.* **1996**, *179*, 211.
(22) Gragson, D. E.; McCarty, B. M.; Richmond, G. L. *J. Phys. Chem.* **1996**, *100*, 14727. Gragson, D. E.; McCarty, B. M.; Richmond, G. L. *J. Am. Chem. Soc.* **1997**, *119*, 6144.
(23) (a) Bain, C. D. *J. Chem. Soc., Faraday Trans.* **1995**, *91*, 1281−96. (b) Miranda, P. B.; Shen, Y. R. *J. Phys. Chem. B* **1999**, *103*, 3292−3307. (c) Shen, Y. R. *Pure Appl. Chem.* **2001**, *73*, 1589−1598. (d) Richmond, G. L. *Annu. Rev. Phys. Chem.* **2001**, *52*, 357−389.
(24) Huh, C.; Reed, R. L. *J. Colloid Interface Sci.* **1983**, *91*, 472.
(25) Rotenberg, Y.; Barouka, L.; Neumann, A. W. *J. Colloid Interface Sci.* **1983**, *93*, 169.
(26) http://www.ekspla.com/products/SFG/sfg1.htm.
(27) (a) Wilson, A.; Epstein, M. B.; Ross, J. *J. Colloid Sci.* **1957**, *12*, 345. Nilsson, G. *J. Phys. Chem.* **1957**, *61*, 1135−1142. (b) Tajima, K.; Muramatsu, M.; Sasaki, T. *Bull. Chem. Soc. Jpn.* **1969**, *42*, 2471.
(28) MacPhail, R. A.; Strauss, H. L.; Snyder, R. G.; Elliger, C. A. *J. Phys. Chem.* **1984**, *88*, 334.
(29) Shen, Y. R. In *Frontiers in Laser Spectroscopy*; Proceedings of the International School of Physics ''Enrico Fermi,'' Course CXX; Hänsch, T., Inguscio, M., Eds. North-Holland: Amsterdam, 1994; pp 139−165.
(30) (a) Bell, G. R.; Bain, C. D.; Ward, R. N. *J. Chem. Soc., Faraday Trans.* **1996**, *92*, 515−523. (b) Ward, R. N.; Duffy, D. C.; Davies, P. B.; Bain, C. D. *J. Phys. Chem.* **1994**, *98*, 8536−8542.
(31) Jedlovszky, P.; Varga, I.; Gilányi, T. *J. Chem. Phys.* **2003**, *119*, 1731−1740.